Telling Tails In The Presence Of A Cosmological Constant

Patrick R. Brady,[(1)] Chris M. Chambers,[(2)] William Krivan,[(3,4)], and Pablo Laguna [(4)]
[(1)] *Theoretical Astrophysics, Mail-Code 130-33, California Institute of Technology, Pasadena, CA 91125*
[(2)] *Department of Physics, Montana State University, Bozeman, MT 59717*
[(3)] *Institut für Astronomie und Astrophysik, Universität Tübingen, D-72076 Tübingen, Germany*
[(4)] *Department of Astronomy & Astrophysics and Center for Gravitational Physics & Geometry, Pennsylvania State University, University Park, PA 16802*
(February 7, 2008)

arXiv:gr-qc/9611056v1 24 Nov 1996

We study the evolution of massless scalar waves propagating on spherically symmetric spacetimes with a non-zero cosmological constant. Considering test fields on both Schwarzschild-de Sitter and Reissner-Nordström-de Sitter backgrounds, we demonstrate the existence of *exponentially* decaying tails at late times. Interestingly the $\ell = 0$ mode asymptotes to a non-zero value, contrasting the asymptotically flat situation. We also compare these results, for $\ell = 0$, with a numerical integration of the Einstein-scalar field equations, finding good agreement between the two. Finally, the significance of these results to the study of the Cauchy horizon stability in black hole-de Sitter spacetimes is discussed.

I. INTRODUCTION

Perturbative studies of relativistic, spherical collapse have elucidated dynamical features of gravitational collapse important to an understanding of black hole formation and the subsequent relaxation to a stationary state (see for example [1]). Indeed, quasi-normal ringing could provide direct evidence of the existence of black holes if observed [2]. At late times, quasi-normal oscillations are swamped by the radiative tail of the gravitational collapse [3]. This tail radiation is of interest in its own right since it originates from the non-trivial propagation of the field perturbations on the background spacetime—zero rest-mass fields do not necessarily propagate along the light-cone in a curved spacetime.

The first authoritative study of nearly spherical collapse, exhibiting radiative tails, was performed by Price [3]. Studying the behaviour of a massless scalar field propagating on a fixed Schwarzschild background, he showed that the field dies off with the now familiar power-law tail $t^{-(2\ell+P+1)}$ at late times, where ℓ is the multipole order of the field, and $P = 1$ if the field is initially static and $P = 2$ otherwise. Furthermore, Price showed that the perturbations of any zero rest-mass, integer-spin field are governed by a wave equation with the same qualitative form as that governing the scalar field. This suggests that the results for the scalar field should apply equally well to the radiatable multipoles of both the electromagnetic and gravitational fields. Similar results for a massless scalar field propagating on a Reissner-Nordström background have been obtained by Bičák [4]. No such analytic result has yet been obtained for the case of a black hole with angular momentum, though Krivan *et al.* [5] have recently performed numerical work which suggests the power law tail holds independently of the angular momentum of the black hole.

While test-field calculations are extremely compelling, it is natural to ask to what extent linear analyses are representative of dynamical gravitational collapse. If either quasi-normal ringing, or radiative tails, should be absent in non-linear collapse one might view results of linear analyses with scepticism. Advances in numerical relativity make it possible to address this issue in the spherically symmetric context. Gómez and Winicour [6] studied the non-linear evolution of a self-gravitating, spherically symmetric, massless scalar field concluding that the scalar monopole moment decayed exponentially rather than with the power-law predicted by the linear analyses. More recently, Gundlach, Price and Pullin [7,8] re-examined this problem. They were able to show that the frequencies of quasi-normal oscillations, and decay rates of the power-law tails, found in the numerical solutions, are in good agreement with the predictions of perturbation theory (though one must go to sufficiently late times in order to see tail effects – this would, in part, explain the null result of Gómez and Winicour).

The presence, and slow decay, of wave tails at late times is a key ingredient leading to the instability of Cauchy horizons inside charged and rotating black holes. For black holes in asymptotically flat spacetime, the inverse power-law decay of perturbing fields at the event horizon has been used to provide initial data in linear [9] and non-linear [10–13] studies of the black hole interior. In particular, the form of the wave tail is largely responsible for the weakness of the mass-inflation singularity inside charged black holes [11], and is believed to have similar consequences inside rotating holes [12].

In contrast to the asymptotically flat case, perturbative [14–16] and non-linear [17] studies indicate that the inner Cauchy horizon of charged and rotating black holes immersed in asymptotically de Sitter space can be stable. That stability persists for a finite volume of the parameter space suggests that these spacetimes violate the letter (if not the spirit) of the cosmic censorship hypothesis [18]. The nature of the radiative tail of perturbations at late times plays a major role in these analyses. Plausible ar-

guments suggest that an exponential decay of the tails replaces the power law behaviour observed in asymptotically flat space [15,16], however, no detailed analysis of the evolution of wave tails in asymptotically de Sitter-black hole spacetimes exists. The present work reports on such a study for non-rotating black holes. Our primary motivation has been to obtain correct boundary conditions on the radiation at the event horizon for use in a numerical study of the internal structure of charged black holes in de Sitter space [16].

The paper is organized as follows: In section II we consider the propagation of massless, minimally coupled scalar fields on the Schwarzschild-de Sitter and Reissner-Nordström-de Sitter black-hole backgrounds. We derive the equation governing the scalar test-field, and numerically integrate it. Two independent numerical codes were used throughout the linear analysis; a null evolution scheme following that of Gundlach *et al.* [7], and a Cauchy evolution scheme similar to that described by Krivan *et al.* [5]. We found complete agreement between them. Our results show that, except for the $\ell = 0$ mode, the field falls off exponentially at the cosmological and black-hole event horizons, and at future timelike infinity. The rate of decay depends upon the surface gravity, κ_1, of the cosmological horizon [see Eq. (9)], and the multipole order of the field. In particular, as $t \to \infty$

$$\phi \sim e^{-\ell \kappa_1 t} \quad , \quad \ell > 0 \, , \tag{1}$$

where t is defined by Eq. (3). For $\ell = 0$, the field approaches a constant value at late times rather than decaying. A suggestion of this behaviour can be found in the analysis of Chambers and Moss [16] and, as argued there, is similar to the situation within the black hole interior. In section III, we study the non-linear evolution of a spherically symmetric, self-gravitating scalar field by numerically integrating the coupled Einstein-scalar field equations. Confining attention to spherical symmetry implies we gain information solely about the $l = 0$ mode of the field. We find, in accord with our linear analysis, that the field approaches a constant value at the cosmological event horizon, the black hole event horizon and future timelike infinity, demonstrating that the results of our linear analysis are indicative of the full theory. Further to this, we inspect the behaviour of the field's stress-energy, showing that

$$\phi_{,r} \sim e^{-2ku} \, , \tag{2}$$

with $k \simeq \kappa_1$ to within about 12%. In section IV we make some final comments about the implications of our results for Cauchy horizon stability in black-hole-de Sitter spacetimes and the related issue of cosmic censorship.

II. A LINEAR ANALYSIS

In this section, we consider a massless, minimally coupled, scalar field propagating on a fixed Reissner-Nordström-de Sitter background. Since our considerations are limited to the black hole exterior, it is clear that the Schwarzschild-de Sitter case can always be obtained by setting the charge $q = 0$ (when this fails, we explicitly include the corresponding formulae).

A. The equations

The generalization of the Reissner-Nordström metric to include a cosmological constant was first given by Carter [19] as

$$ds^2 = -f(r)dt^2 + f(r)^{-1}dr^2 + r^2(d\theta^2 + \sin^2\theta d\phi^2) \, , \tag{3}$$

where

$$f(r) = 1 - \frac{2M}{r} + \frac{q^2}{r^2} - \frac{r^2}{\alpha^2} \quad , \quad \alpha^2 = \frac{3}{\Lambda} > 0 \, . \tag{4}$$

In Eq.(4), M denotes the mass of the black hole, q its charge and Λ is the cosmological constant. If $q \neq 0$ there are three horizons located at the roots of $f(r) = 0$; an inner (Cauchy) horizon at $r = r_3$, a black hole event horizon at $r = r_2$ and a cosmological horizon located at $r = r_1$ such that $r_1 > r_2 > r_3$ (see Fig. 2). The fourth root, r_4, is negative and thus non-physical. (When $q = 0$ there are only two horizons (see Fig. 1) the black hole event horizon, r_2, and the cosmological event horizon, r_1, while the third root, r_3 is negative.)

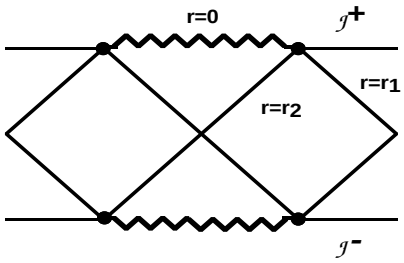

FIG. 1. A conformal diagram representing the Schwarzschild-de Sitter black hole spacetime. Shown are the cosmological horizon at $r = r_1$, the black hole event horizon at $r = r_2$ and the singularity (wavy line) located at $r = 0$. Also shown are the locations of past and future null infinity $\mathcal{J}^-$ and $\mathcal{J}^+$ respectively.

It is convenient to introduce a “tortoise” radial coordinate, $r_* = \int dr/f(r)$, which takes the explicit form

$$r_* = \begin{cases} -\frac{1}{2\kappa_1}\ln\left|\frac{r}{r_1}-1\right| + \frac{1}{2\kappa_2}\ln\left|\frac{r}{r_2}-1\right| - \frac{1}{2\kappa_3}\ln\left|\frac{r}{r_3}-1\right| + \frac{1}{2\kappa_4}\ln\left|\frac{r}{r_4}-1\right| \quad , \quad q \neq 0 \, , \\ -\frac{1}{2\kappa_1}\ln\left|\frac{r}{r_1}-1\right| + \frac{1}{2\kappa_2}\ln\left|\frac{r}{r_2}-1\right| + \frac{1}{2\kappa_3}\ln\left|\frac{r}{r_3}-1\right| \quad , \quad q = 0 \, , \end{cases} \tag{5}$$

where the arbitrary constant of integration has been set to zero.

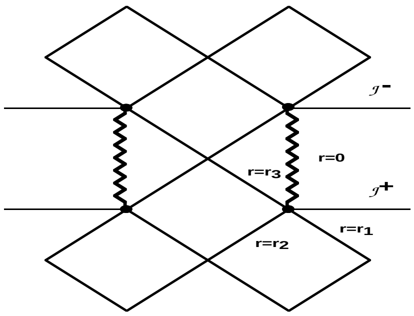

FIG. 2. A conformal diagram showing the Reissner-Nordström-de Sitter black hole spacetime. Shown are the cosmological horizon at $r = r_1$, the black hole event horizon at $r = r_2$, the inner (Cauchy) horizon at $r = r_3$ and the singularity (wavy line) located at $r = 0$. Past and future null infinity are indicated by $\mathscr{J}^-$ and $\mathscr{J}^+$ respectively.

We define

$$\kappa_i = \frac{1}{2}\left|\frac{df(r)}{dr}\right|_{r=r_i} \, , \tag{6}$$

where r_i are the roots of $f(r) = 0$. When the root corresponds to a physical horizon in the spacetime, κ_i is the surface gravity of that horizon [20]. Finally, we introduce a pair of null coordinates on the spacetimes, the advanced time $v = t + r_*$ and the retarded time $u = t - r_*$, in terms of which the interval (3) reduces to,

$$ds^2 = -f(r)dudv + r^2(d\theta^2 + \sin^2\theta d\phi^2) \, . \tag{7}$$

The definition we have adopted means that the future cosmological horizon $r = r_1$ is located at $v = \infty$, and the future black-hole event horizon $r = r_2$ is at $u = \infty$. In terms of the null coordinates (u, v), the scalar wave equation, $\Box\phi = 0$, becomes

$$\Psi_{,uv} = -\frac{1}{4}V_\ell(r)\Psi \tag{8}$$

where we have decomposed the field into its constituent multipole pieces, i.e. $\phi = \sum \Psi(u,v)Y_{\ell m}(\theta,\phi)r^{-1}$. The effective potential

$$V_l(r) = f(r)\left(\frac{\ell(\ell+1)}{r^2} + \frac{2M}{r^3} - \frac{2q^2}{r^4} - \frac{2}{\alpha^2}\right) \, , \tag{9}$$

is highly localized near to $r_* = 0$, falling off exponentially in r_* at both $r = r_1$ and $r = r_2$. The form of the potential for $\ell = 0, 1$ and $\ell = 2$ is shown in Fig. 3.

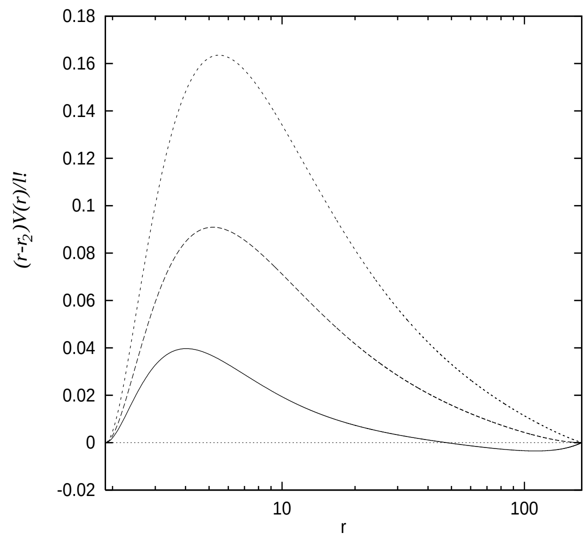

FIG. 3. The ‘effective’ potential when $q = 0.5$, $M = 1$, $\Lambda = 10^{-4}$ and $\ell = 0$ (solid), $\ell = 1$ (dashed) and $\ell = 2$ (dotted). We have multiplied by $|r - r_2|/\ell!$ in order to accentuate the nature of the potential when $\ell = 0$—the usual potential barrier is followed by a potential well, a feature not evident when $\ell > 0$. The potential tends to zero exponentially quickly as $r_* \to \pm\infty$.

B. The results

It is straightforward to integrate Eq.(8) on a null grid using the methods described by Gundlach *et al.* [7]. Further details can be found in their article.

Since tail effects are independent of the initial data used, we chose to represent a generic initial perturbation by a Gaussian pulse on $u = 0$

$$\Psi(u = 0, v) = A\exp\{-(v - v_1)^2/\sigma^2\} \, . \tag{10}$$

(The amplitude A is irrelevant since Eq. (8) is linear. The data used to produce the figures had center $v_1 = 50.0$, and width $\sigma = 3.0$.) The field is constant on $v = 0$, $\Psi(v = 0) = \Psi(u = 0, v = 0)$. We have set the mass of the hole, M, equal to unity throughout; this corresponds to the freedom to rescale the coordinates by an overall length scale. Investigations have shown that the results are qualitatively similar for all $\Lambda > 0$, so we fix $\Lambda = 10^{-4}$ from here on. We discuss the behaviour of the field, $\phi = \Psi/r$, in three regions: (a) timelike infinity—approached

on surfaces of constant r. (b) The cosmological horizon—in practice, approximated by the null surface $v = v_{\max}$, the largest value of v on our grid. (c) The black-hole event horizon—again, approximated by the null surface $u = u_{\max}$, the largest value of u on our grid.

Gundlach *et al.* [7] argued that the nature of the tails in asymptotically flat spacetimes is primarily due to the power-law form of the effective potential as $r_* \to \infty$. Moreover, Ching *et al.* [21] have demonstrated that inverse power-law tails, as seen in spherically symmetric, asymptotically flat spacetimes, are not generic. Therefore, it should not be surprising that tails, in asymptotically de Sitter spacetimes, fall off exponentially with time since the effective potential is exponentially suppressed as $r_* \to \pm\infty$. What is unexpected is that the the $\ell = 0$ modes do not decay to zero, rather a generic perturbation leads to a residual constant field at late times. (Of course, there is no stress-energy associated with a constant field.) This was suggested in a paper by Chambers and Moss [16] where it was argued that the situation in Schwarzschild-de Sitter spacetime is somewhat analogous to scattering inside a black hole [9], and hence a constant mode can be transmitted to both the black-hole and cosmological event horizons. Indeed, the field at late times behaves like

$$\phi|_{l=0} \simeq \phi_0 + \phi_1(r)e^{-2\kappa_1 t} \ . \tag{11}$$

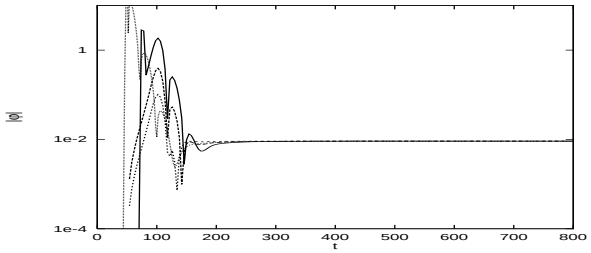

FIG. 4. A plot of $|\phi|$ versus time for $q = 0.5$, $\ell = 0$, $M = 1$ and $\Lambda = 10^{-4}$. The field is shown on the cosmological event horizon r_1 (short-dashed), the black hole event horizon r_2 (dotted) and two surfaces of constant radius (solid and long-dashed). Initially the quasi-normal ringing dominates, while at late times the field settles down to the same constant value on all four surfaces.

Figure 4 demonstrates this effect. The early time behaviour of the field, ϕ, is dominated by the quasi-normal ringing, whose explicit features we are not currently interested in. At later times the field quickly approaches the same constant value at the cosmological event horizon, the black-hole event horizon and future timelike infinity.

One might suspect that the existence of a non-zero field at late times is an artifact of the initial data, or that setting $q = 0$ might produce different results. Therefore Fig. 5 shows results for a Schwarzschild-de Sitter black hole with $\ell = 0$. Once again, the field settles down to a constant value which is independent of the radial position. One must contrast this to previous results for asymptotically flat spacetimes where the field always approaches zero. Monitoring the behaviour of $\phi_{,t}$ during the evolution (this is a matter of formality in the Cauchy code, as it uses momenta $p_t = \phi_{,t}$ for the evolution) has allowed us to conclude that the numerical value of the exponent in Eq.(11) is indeed κ_1 to within 10%: Taking the time derivative of Eq.(11) yields $\ln|\phi_{,t}| = \ln(2\kappa_1\phi_1(r)) - 2\kappa_1 t$, thus the fitted values for κ_1 can be compared with the ones obtained from Eq.(6).

In general, the final field value, ϕ_0, is a function of the black hole parameters (M, q, Λ). We investigated the dependance of ϕ_0 on the cosmological constant Λ. As shown in Fig. 6 for the case $q = 0, M = 1$, our results indicate that $\phi_0 \sim \Lambda^{0.6}$. The linear correlation coefficient $c_{\rm lin}$ of $\ln|\phi_0|$ versus $\ln\Lambda$ is given by $c_{\rm lin} = 0.98$.

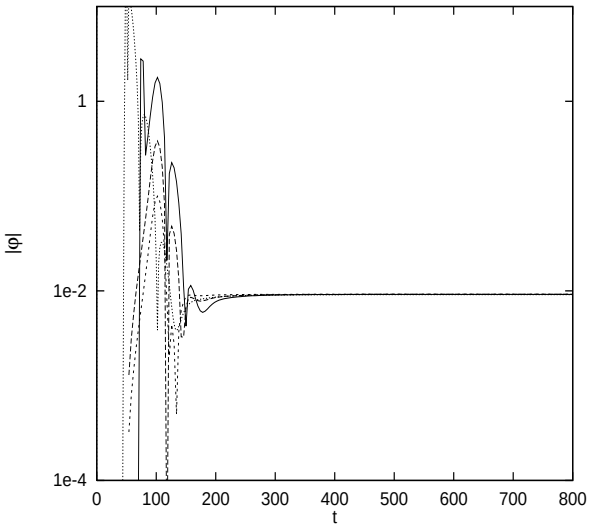

FIG. 5. A plot of $|\phi|$ versus time when $q = 0.0$, $\ell = 0$, $M = 1$ and $\Lambda = 10^{-4}$. The field is exhibited on the same surfaces as the $q = 0.5$ cases. Once again the asymptotically constant field is evident.

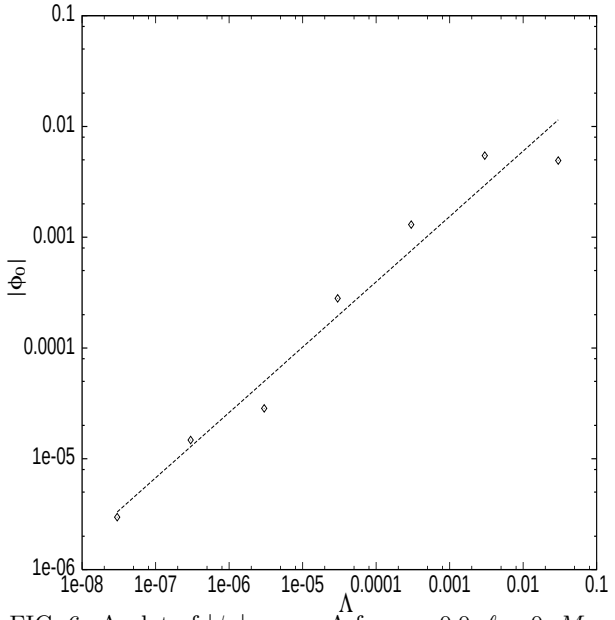

FIG. 6. A plot of $|\phi_0|$ versus Λ for $q = 0.0$, $\ell = 0$, $M = 1$. The linear correlation coefficient $c_{\rm lin}$ of $\ln|\phi_0|$ versus $\ln\Lambda$ is given by $c_{\rm lin} = 0.98$. The dashed line represents the least square fit to $|\phi_0| = b\,\Lambda^a$ with $a = 0.59$, $b = 0.09$.

For $\ell > 0$ the picture is different, as seen from Fig. 7 and Fig. 8. The early time behaviour of the field is still dominated by complicated quasi-normal ringing, but at late times a definite exponential fall-off is manifest. In particular, the late time wave tails are well approximated by $\phi|_\ell \sim \exp(-\ell\kappa_1 t)$. In a series of separate evolutions we found that for sufficiently small values of Λ, a regime of power law decay followed the quasi-normal ringing, though at late times the exponential decay described above always dominates.

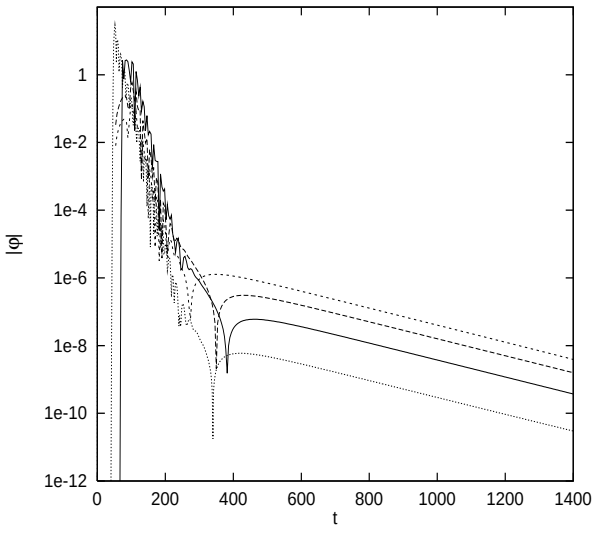

FIG. 7. A plot of $|\phi|$ versus time for $q = 0.5$, $\ell = 1$, $M = 1$ and $\Lambda = 10^{-4}$. The field along is shown on the cosmological event horizon r_1 (short-dashed), the black hole event horizon r_2 (dotted) and two surfaces of constant radius (solid and long-dashed). The field falls off as $\exp(-kt)$ at late times, with $k \simeq \kappa_1$ to within about 2%. Note that the ordinate scale is logarithmic.

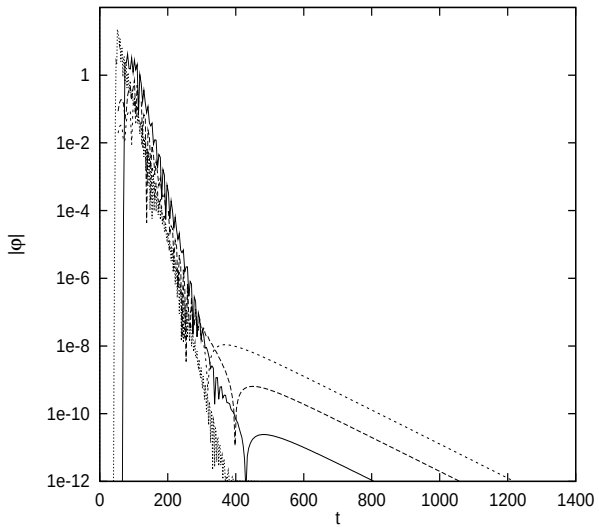

FIG. 8. A plot of $|\phi|$ versus time for $q = 0.5$, $\ell = 2$, $M = 1$ and $\Lambda = 10^{-4}$. The field is shown on the cosmological event horizon r_1 (short-dashed), the black hole event horizon r_2 (dotted) and two surfaces of constant radius (solid and long-dashed). At early times quasi-normal ringing completely dominates, but eventually the field falls off as $\exp(-2kt)$. The value of $k \simeq \kappa_1$ is again accurate to approximately 2%. Note that the ordinate scale is logarithmic.

III. NON-LINEAR ANALYSIS

Given the somewhat unusual behaviour of the $\ell = 0$ modes elucidated by the test field analysis, it seems necessary to examine the non-linear evolution of a self-gravitating massless, scalar field in the presence of a cosmological constant. This situation is described by the coupled Einstein-scalar field equations

$$G_{\alpha\beta} = 8\pi T_{\alpha\beta} - g_{\alpha\beta}\Lambda\ , \tag{12}$$

where

$$T_{\alpha\beta} = \phi_{,\alpha}\phi_{,\beta} - (1/2)g_{\alpha\beta}(\phi_{,\gamma}\phi^{,\gamma})\ , \tag{13}$$

is the stress-energy of the scalar field which satisfies $\Box\phi = 0$. Restricting attention to spherical symmetry (thus we only gain information about the $\ell = 0$ mode) the line element can be written as

$$ds^2 = -g\bar{g}du^2 - 2gdudr + r^2(d\theta^2 + \sin^2\theta d\phi^2)\ , \tag{14}$$

where $g = g(u,r)$, $\bar{g} = \bar{g}(u,r)$ and u is the retarded time. The coordinates have been normalized so that u is the

proper time at the origin, thus $g(0,r) = \bar{g}(0,r) = 1$. It is customary [22] to introduce two new fields $\bar{h}(u,r)$ and $h(u,r)$ defined by

$$\phi = \bar{h} = \frac{1}{r}\int_0^r h\, dr\ . \tag{15}$$

In terms of these variables the field equations (12) become

$$(\ln g)_{,r} = 4\pi r^{-1}(h-\bar{h})^2\ , \tag{16}$$

$$(r\bar{g})_{,r} = g(1-\Lambda r^2)\ , \tag{17}$$

$$(r\bar{h})_{,r} = h\ , \tag{18}$$

and the wave equation is

$$h_{,u} - \frac{\bar{g}}{2}h_{,r} = \frac{(h-\bar{h})}{2r}\left[g(1-\Lambda r^2) - \bar{g}\right]\ . \tag{19}$$

A well established numerical algorithm exists to integrate these equations [8,23,24]. We refer the reader to these articles for details.

A. The results

Initial data for the non-linear equations is supplied on an initial null cone centered on the origin. We considered a Gaussian pulse on $u = 0$, with an amplitude $\phi_0(r/r_0)^2$, width σ, and centered on $r = r_0$. The code was tested against the exact solution in [25]. We also reproduced power-law tails in complete agreement with [8], when $\Lambda = 0$.

Figure 9 shows $\bar{h}$ (or equivalently ϕ) at the cosmological event horizon, the black hole event horizon and along an $r = constant$ surface. The agreement with the linear analysis is remarkable. We again see an initial period of quasi-normal ringing which decays, leaving behind a constant field at late times.

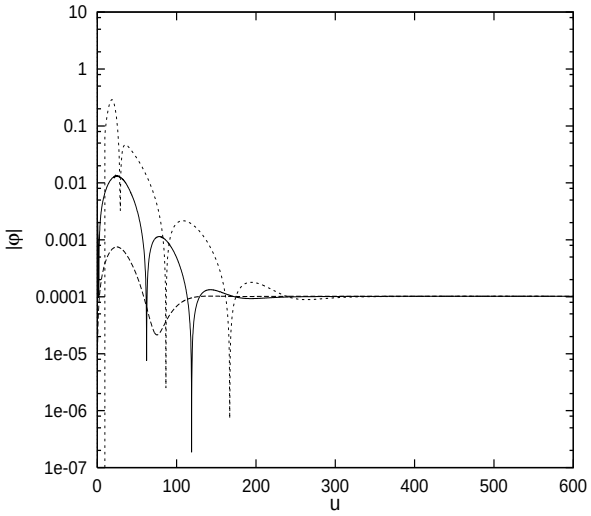

FIG. 9. A plot of $|\phi|$ versus time for $\Lambda = 10^{-4}$. The field is shown along three surfaces: the cosmological event horizon r_1 (short-dashed), the black hole event horizon r_2 (long-dashed) and a surface of constant radius (solid). After a period of quasi-normal ringing the field settles down to the same constant value at all three surfaces.

Furthermore, using (15) and (18) we can write $r\phi_{,r} = (\bar{h} - h)$ and examine the stress-energy of the field at late times. Figure 10 suggests that $(\bar{h} - h) \sim \exp[-2\kappa_1 u]$ at late times, as suggested by the the test-field analysis.

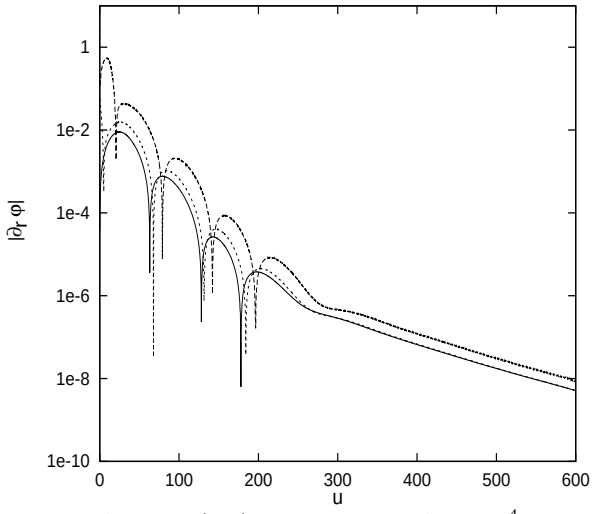

FIG. 10. A plot of $|\phi_{,r}|$ versus time for $\Lambda = 10^{-4}$ along the same three surfaces. At late times exponential decay with the approximate form $\exp(-2ku)$ is evident—we have determined the value of $k \simeq \kappa_1$ within about 12%.

IV. CONCLUDING REMARKS

This study of wave-tail evolution in black hole-de Sitter spacetimes has revealed consistent but interesting results. The radiative tails associated with a massless, minimally coupled scalar field propagating on the fixed backgrounds of a Schwarzschild-de Sitter and Reissner-Nordström-de Sitter black hole decay exponentially at the cosmological horizon, the black hole event horizon and at future timelike infinity. That is, for all modes except the $\ell = 0$ mode, it approaches a constant at late times. We have further explored this result by considering the non-linear problem of a scalar field coupled to gravity and numerically integrating the Einstein-scalar field equations. These results show excellent agreement with the linear analysis.

Though the introduction of a non-zero cosmological constant into the Einstein equations may be argued to be somewhat unrealistic, it is the issue of Cauchy horizon stability in black hole-de Sitter spacetimes [14–16] and the related issue of cosmic censorship [18], that motivates this investigation. The power-law tails found by Price [3] have been used as initial data in arguments pertaining

to the instability of the inner (Cauchy) horizon of both the Reissner-Nordström and Kerr black hole spacetimes and the associated phenomenon of mass inflation. Linear perturbation studies suggest that the Cauchy horizon inside black holes embedded in de Sitter space may be stable—fluxes of linear perturbations remain bounded at the Cauchy horizon. This in itself does not guarantee stability though. A fully non-linear analysis of the black hole interior is needed, for which the late-time wave tails at the event horizon serve as initial data. With the results of this paper in hand, we can now embark on a numerical study of the Cauchy horizon in Reissner-Nordström-de Sitter, along the lines of Brady and Smith [13].

ACKNOWLEDGMENTS

PRB is grateful to Bruce Allen and Kip Thorne for helpful discussions. CMC wishes to thank the Caltech Relativity Group for hospitality during the completion of this work and the Relativity group at Montana State University for their constant support over the last year. CMC is a Fellow of The Royal Commission For The Exhibition Of 1851 who's financial support is gratefully acknowledged. PRB is supported by a PMA Division Fellowship at Caltech and NSF Grant AST-9417371. WK is supported by the Deutscher Akademischer Austauschdienst (DAAD). PL is supported by the Binary Black Hole Grand Challenge Alliance, NSF PHY/ASC 9318152 (ARPA supplemented) and by NSF grants PHY 96-01413, 93-57219 (NYI).

[1] C.W. Misner, K.S. Thorne and J.A. Wheeler, *Gravitation* (Freeman, San Francisco 1973).
[2] K.S. Thorne, in *300 Years of Gravitation*, ed. S.W. Hawking and W. Israel (Cambridge University Press, 1987).
[3] R.H. Price, Phys. Rev. D **5**, 2419 (1972); Phys. Rev. D **5**, 2439 (1972).
[4] J. Bičák, Gen. Relativ. Gravit. **3**, 331-349 (1972).
[5] W. Krivan, P. Laguna and P. Papadopoulos, Phys. Rev. D **54**, 4728 (1996).
[6] R. Gómez and J. Winicour, J. Math. Phys. **33**, 1445 (1992).
[7] C. Gundlach, R.H. Price and J. Pullin, Phys. Rev. D **49**, 883 (1994).
[8] C. Gundlach, R.H. Price and J. Pullin, Phys. Rev. D **49**, 890 (1994).
[9] S. Chandrasekhar and J.B. Hartle, Proc. R. Soc. London **A 284**, 301 (1982); M. Simpson and R. Penrose, Int. J. Theor. Phys. **7**, 183 (1973); Y. Gursel, V.D. Sandberg, I.D. Novikov and A.A. Starobinsky, Phys. Rev. D **19** 413 (1979); Phys. Rev. D **20** 1260 (1979).
[10] W. Israel and E. Poisson, Phys. Rev. D **41**, 1796 (1990); A. Bonnano, S. Droz, W. Israel and S.M. Morsink, Can. J. Phys **72**, 755 (1994) and references therein.
[11] A. Ori, Phys. Rev. Lett. **67**, 789 (1991); R. Balbinot, P.R. Brady, E. Poisson and W. Israel, Phys. Lett. **A161**, 223 (1991).
[12] A. Ori, Phys. Rev. Lett. **68**, 2117 (1992); P.R. Brady and C.M. Chambers, Phys. Rev. D **51**, 4177 (1995); P.R. Brady, S. Droz, W. Israel and S.M. Morsink (paper in preparation).
[13] P.R. Brady and J.D. Smith, Phys. Rev. Lett. **75**, 1256 (1995).
[14] F. Mellor and I.G. Moss, Phys. Rev. D **41**, 403 (1990); Class. Quantum Grav. **9**, L43 (1992); C.M. Chambers and I.G. Moss, Class. Quantum Grav. **11**, 1035 (1994).
[15] P.R. Brady and E. Poisson, Class. Quantum Grav. **9**, 121 (1992).
[16] C.M. Chambers and I.G. Moss, Phys. Rev. Lett. **73**, 617 (1994).
[17] P.R. Brady, D. Núñez and S. Sinha, Phys. Rev. D **47**, 4239 (1993).
[18] See R. Penrose, in *Battelle Rencontres*, ed. C.M. DeWitt and J.A. Wheeler (W.A. Benjamin, New York, 1968), for a discussion on the relationship between Cauchy horizon instability and the cosmic censorship hypothesis.
[19] B. Carter, in *Black Holes*, ed. C.M. DeWitt and B.S. DeWitt (Gordon and Breach, New York, 1973).
[20] R.M. Wald, *General Relativity* (The University of Chicago Press, Chicago 1984), chapter 12.
[21] E.S.C. Ching, P.T. Leung, W.M. Suen and K. Young, Phys. Rev. Lett. **74**, 2414 (1995).
[22] D. Christodoulou, Comm. Math. Phys. **105**, 337 (1986).
[23] D.S. Goldwirth and T. Piran, Phys. Rev. D **36**, 3575 (1987).
[24] D. Garfinkle, Phys. Rev. D **51**, 5558 (1995).
[25] P.R. Brady, Class. Quantum Gravity **11**, 1255 (1994).